Ultrasonographic morphological characteristics determined using a deep learning-based computer-aided diagnostic system of breast cancer

Young Seon Kim, MD[a],* , Seung Eun Lee, MD[a], Jung Min Chang, MD, PhD[b], Soo-Yeon Kim, MD, PhD[b], Young Kyung Bae, MD, PhD[c]

Abstract

To investigate the correlations between ultrasonographic morphological characteristics quantitatively assessed using a deep learning-based computer-aided diagnostic system (DL-CAD) and histopathologic features of breast cancer.

This retrospective study included 282 women with invasive breast cancer (<5 cm; mean age, 54.4 [range, 29–85] years) who underwent surgery between February 2016 and April 2017. The morphological characteristics of breast cancer on B-mode ultrasonography were analyzed using DL-CAD, and quantitative scores (0–1) were obtained. Associations between quantitative scores and tumor histologic type, grade, size, subtype, and lymph node status were compared.

Two-hundred and thirty-six (83.7%) tumors were invasive ductal carcinoma, 18 (6.4%) invasive lobular carcinoma, and 28 (9.9%) micropapillary, apocrine, and mucinous. The mean size was 1.8 ± 1.0 (standard deviation) cm, and 108 (38.3%) cases were node positive. Irregular shape score was associated with tumor size (P < .001), lymph nodes status (P = .001), and estrogen receptor status (P = .016). Not-circumscribed margin (P < .001) and hypoechogenicity (P = .003) scores correlated with tumor size, and non-parallel orientation score correlated with histologic grade (P = .024). Luminal A tumors exhibited more irregular features (P = .048) with no parallel orientation (P = .002), whereas triple-negative breast cancer showed a rounder/more oval and parallel orientation.

Quantitative morphological characteristics of breast cancers determined using DL-CAD correlated with histopathologic features and could provide useful information about breast cancer phenotypes.

Abbreviations: BI-RADS = breast imaging-reporting and data system, DL-CAD = deep learning-based computer-aided diagnosis, ER = estrogen receptor, HER2 = human epidermal growth factor receptor 2, IHC = immunohistochemical, LN = lymph nodes, MG = mammography, MRI = magnetic resonance imaging, PR = progesterone receptor, ROI = region of interest, TNBC = triple-negative breast cancer, US = ultrasonography.

Keywords: breast cancer subtype, deep learning algorithm, invasive breast cancer, morphological characteristics, ultrasound

1. Introduction

Breast cancer is the most commonly diagnosed cancer and the leading cause of cancer-related deaths in women worldwide.[1] Histopathologic evaluation of breast cancer by tissue sampling is essential for treatment planning and prediction of prognosis, and it provides information on the tumor size, histologic grade, nodal status, expression of estrogen receptor (ER), progesterone receptor (PR), and human epidermal growth factor receptor 2

[a] Department of Radiology, Yeungnam University Hospital, Yeungnam University College of Medicine, Daegu, South Korea, [b] Department of Radiology, Seoul National University Hospital, Seoul, South Korea, [c] Department of Pathology, Yeungnam University Hospital, Yeungnam University College of Medicine, Daegu, South Korea.

* Correspondence: Young Seon Kim, Department of Radiology, College of Medicine, Yeungnam University, 170, Hyeonchung-ro, Nam-gu, Daegu 42415, South Korea (e-mail: youngseon29@gmail.com).

(HER2), which are very important prognostic markers.[2,3] Recent advances in image acquisition, computational power, and algorithmic development have allowed quantitative information acquisition from computer-aided diagnosis.[4–8] Imaging techniques have been shown to non-invasively provide information regarding the underlying histopathology,[9] and this technology has been adopted previously to phenotypically characterize breast cancers using preoperative magnetic resonance imaging (MRI).[10–12]

Ultrasound (US) has many advantages such as ease of accessibility without the need for radiation and contrast material. Recently, high-resolution US has proven useful for the evaluation of small structures, such as nerves or tendons, and its diagnostic accuracy is comparable to that of MRI.[13,14] US is a widely used imaging modality for breast cancer detection in adjunct to mammography (MG) in women with dense breasts and breast mass differentiation.[15] In breast cancer evaluation, US can be used to assess the extent, multifocality, and multicentricity of the tumor in the breast, and axillary lymphadenopathy.[16–18] Besides, US is useful for the treatment response monitoring of breast cancer.[19,20] However, US has some limitations, including operator dependency and limited reproducibility. Consequently, quantitative and objective analyses of morphological characteristics with US are limited, and the correlation between breast cancer and histopathologic features has not been well investigated.

Recent advances in artificial intelligence, particularly deep learning algorithms, have gained extensive attention owing to their excellent performance in image recognition tasks.[21] It can be used to detect subtle findings in US images that expert radiologists overlook and automatically produce a quantitative assessment.[7,8] Deep learning-based computer-aided diagnosis (DL-CAD) software for breast US has been developed and applied in clinical practice, and its assistance in the morphological analysis of breast masses has improved diagnostic accuracy and sensitivity.[8,22–24] A recently developed, commercially available DL-CAD software for breast US (S-Detect; Samsung Medison Co., Seongnam, Korea) provides computer-based analysis of breast tumors based on morphologic features using a novel feature extraction technique and support vector machine classifier that provides a dichotomized final assessment of breast mass, possibly benign or possibly malignant, based on the American College of Radiology Breast Imaging Reporting and Data System ultrasonographic descriptors.[8,25,26]

In addition to lesion differentiation, we assume that the quantitative morphological information regarding breast cancer obtained on US would provide histopathologic information, including molecular subtypes, similar to quantitative radiomics analysis using MRI.[27–30] Previous studies have revealed that irregular shape and spiculated or indistinct margins with posterior acoustic shadowing are associated with the luminal subtype, and oval to round shape and circumscribed margins with posterior acoustic enhancement are common in triple-negative breast cancer (TNBC) on breast US.[31–34] However, the mass characteristics were assessed by qualitatively by radiologist, and quantitative assessment was not performed. The limitations of ultrasound, especially operator dependency, could be reduced by proving an association between quantitative assessment of ultrasound images using DL-CAD and histopathologic features, such as a specific tumor subtype.

Therefore, the purpose of our study was to investigate the correlations between ultrasonographic morphological character-

istics, quantitatively assessed using DL-CAD, and histopathologic features of breast cancer.

2. Methods

2.1. Patients

We present the following article in accordance with the STROBE reporting checklist. The Institutional Review Board of Yeungnam University Hospital (IRB No. 2018-07-016) approved this retrospective study and waived the requirement for informed consent. All the methods in the study involving human participants were performed in accordance with relevant guidelines and regulations of the institutional and/or national research committee and with the 1964 Helsinki declaration and its lateral amendments or comparable ethical standards. Between February 2016 and April 2017, 459 women with newly diagnosed invasive breast cancer (on percutaneous biopsy) who had previously undergone preoperative breast US and subsequent surgery were included through a review of medical records at our institution, a tertiary academic hospital. Women were excluded if they had only ductal carcinoma in situ without invasive cancer on the surgical specimen (n = 84), the tumor was >5 cm (n = 32), had previously undergone neoadjuvant chemotherapy before surgery (n = 52), had previously undergone vacuum-assisted or excisional biopsy for diagnosis before preoperative US (n = 8), and had insufficient immunohistochemical (IHC) results on pathologic reports (n = 1). Only the tumors with the largest dimensions were included in women with multifocal or multicentric breast cancers. Finally, a total of 282 consecutive women (mean age, 54.4 years; range, 29–85 years) were included in our study.

2.2. Ultrasound image acquisition

Preoperative breast US was performed by one of the two board-certified breast radiologists (KYS and HMS with 5 and 25 years of experience in breast imaging, respectively) using iU22 (Philips Medical Systems, Bothell, WA) with a 5 to 12 MHz linear array transducer. All breast ultrasound examinations were performed in real-time with a handheld ultrasound probe, and bilateral whole-breast scanning was conducted. A standardized scanning protocol was used for every examination, using the transverse and sagittal orientations, with the inner aspect of the breast scanned with the patient in a supine position, and the outer aspect in supine oblique position, with the patient's ipsilateral arm raised above the head. The axilla was routinely scanned before the breast in our protocol.

Two additional board-certified breast radiologists (KYS and CJM with 5 and 13 years of experience in breast imaging, respectively) retrospectively reviewed the US images and selected the most representative image with consensus for each tumor for CAD analysis. Following image selection, each image was stored in the DICOM format.

2.3. Pathologic analysis

All patients underwent breast surgery, including breast-conserving surgery (n = 202, 71.6%) or mastectomy (n = 80, 28.4%). We reviewed each patient's pathological report of the surgical specimen to identify the invasive tumor size, histologic grade based on the Elston–Ellis system,[35] histologic types of invasive cancer, lymph node (LN) status, and IHC analysis findings (i.e., ER, PR, and HER2 status, Ki67). For the interpretation of IHC

analysis, semi-quantitative scorings of the percentage of positive cells with nuclear staining (range, 0–100%) was used for ER and PR expression levels. The cutoff value for defining ER and PR positivity was 1%.[36] IHC analysis results were initially used to define HER2 expression, and tumors with a score of 3+ were defined as HER2-positive, and those with a score of 0 or 1+ were defined as HER2-negative. For cases with a score of 2+ on IHC, silver-enhanced in situ hybridization for the HER2 gene was performed to define HER2 expression. The percentage of the total number of tumor cells with nuclear staining was used to define the Ki67 index.[37] Breast cancers were divided into 4 subtypes based on the IHC results: luminal A (ER- and/or PR-positive, HER2-negative, Ki67≤20%), luminal B (ER- and/or PR-positive, either HER2-positive or HER2-negative with Ki67 >20%), HER2-positive (HER2-positive, ER- and PR-negative), and triple-negative (ER-, PR-, and HER2-negative).[38]

2.4. Analysis of quantitative morphologic scores using DL-CAD

A commercially available DL-CAD software (S-Detect; Samsung Medison Co., Seongnam, Korea) for breast US was used to obtain quantitative morphological information on mass features, and the final assessment was performed at a dedicated workstation. It provides computer-based analysis of tumor morphology using a novel feature extraction technique and a support vector machine classifier.[25] The current commercially available version of the DL-CAD software only displays the final assessments in a dichotomized form as "possibly benign" or "possibly malignant" based on the maximum value of each breast imaging-reporting

and data system (BI-RADS) descriptor (shape, margin, orientation, echo pattern, and posterior echogenic features), and does not present the quantitative morphologic scores. However, with technical support from Samsung Medison Co. (Seongnam, Korea), we used the original outputs (quantitative scores) of the DL-CAD software to analyze the US images. In the algorithm used, deep learning technology was applied during the generation of quantitative morphologic scores to build a classifier for BI-RADS descriptors. A series of layers of simple components constitute a network, each having their own nonlinear mappings between the input and output. In contrast to conventional machine learning, where human experts need to select representative imaging features, deep learning algorithms do not require human input. Instead, they determine the manner in which internal parameters are the best representations of data from large high-dimensional datasets via learning procedures.[39] Combining the output for each BI-RADS descriptor with that of the other network for classifying the region of interest (ROI) images results in the final decision.[39–41]

Using DL-CAD software, the radiologists indicated the center of the mass, and a ROI was automatically drawn along the border of the mass. When the mass boundary was inadequately drawn, manual correction was performed. It automatically generated quantitative output values in a range between 0 and 1 for mass shape, orientation, margin, posterior features, and echo pattern for ROI-based masses on US according to the 5th edition of the BI-RADS lexicon (Fig. 1). To simplify the analysis, the internal values of shape, orientation, margin, and echo pattern were collected and arranged in a dichotomized manner (i.e., shape: irregular vs not-irregular, margin: circumscribed vs not-circum-
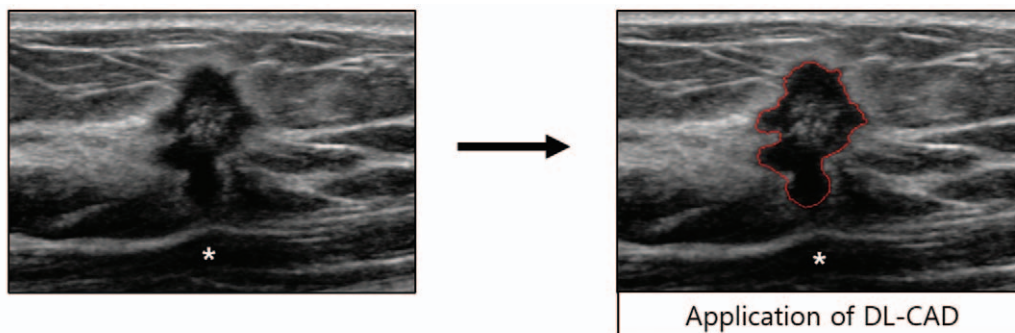
Shape		Margin		Echo pattern		Orientation		Posterior Features	
Round	0.006818	Circumscribed	0	Anechoic	0.001265	Parallel	0.015081	**No**	0.890899
Oval	0.006608	Indistinct	0.000128	Hyperechoic	0	**Not parallel**	0.984919	Enhancement	0.00176
Irregular	0.986574	**Spiculated**	0.999489	Complex	0.002771			Shadowing	0.107318
		Angular	0.000004	**Hypoechoic**	0.994668			Combined	0.000018
		Microlobulated	0.000379	Isoechoic	0.001288				
				Heterogeneous	0.000008				
Results of Quantitative Morphologic Scores by DL-CAD									

Figure 1. Analysis of morphologic score of tumor on US using deep learning based computer-aided diagnosis (DL-CAD) software. A region of interest (ROI) (red line) was automatically drawn along the border of the tumor in a 46-year-old woman, and the US morphologic features were analyzed by the DL-CAD based on the ROI. The table shows quantitative scores of this tumor obtained from DL-CAD software (* pectoralis muscle under the lesion).

scribed, echogenicity: hypoechoic vs not-hypoechoic, orientation: parallel vs not-parallel).

2.5. Data and statistical analysis

The quantitative morphological scores obtained using the DL-CAD software and the histopathological findings of the subsequent surgical specimens of 282 tumors were reviewed. We analyzed the correlation between the pathological features (mass size, tumor histologic grade, LN status, molecular subtype, etc) and quantitative scores of masses for each lexicon on US. The tumors were subdivided into 3 groups according to the size of the mass: <1 cm, 1 to 2 cm, and >2 cm. The quantitative scores of the masses on US were analyzed according to histopathological features using Student t test or one-way analysis of variance. In addition, multiple linear regression analysis with the stepwise selection method was used to determine the relative influence of the different histopathological features on the quantitative scores of masses for each lexicon on US. All statistical analyses were performed using SPSS statistics version 25 for Windows (SPSS Inc., Chicago, IL), and a P value <.05 was considered to indicate a significant difference.

3. Results

3.1. Baseline characteristics

A total of 282 tumors from 282 consecutive women were included in our study. The mean size of the 282 invasive tumors was 1.8 ± 1.0 (standard deviation) cm. For the histologic type of breast cancer, invasive ductal carcinoma, not otherwise specified (IDC, NOS) was the most common histologic type (n=236, 83.7%), followed by invasive lobular carcinoma (ILC) (n=18, 6.4%). There were 192 (68.1%) pathologic T1-stage tumors and 90 (31.9%) T2-stage tumors. Most cases were LN-negative (n= 174, 61.7%). The IHC results showed that luminal A tumors were the most common tumors (n=144, 51.1%), followed by luminal B tumors (n=77, 27.3%), TNBC (n=39, 13.8%), and HER2-positive tumors (n=22, 7.8%). Patient and tumor characteristics are listed in Table 1.

3.2. US morphological characteristics associated with histopathologic features

We analyzed the correlations between US quantitative morphological scores obtained using DL-CAD and pathologic features, including tumor size, tumor histologic grade, LN status, receptor status, and tumor subtype. In the univariate analysis, the irregular shape score on US was higher in tumors with specific pathologic characteristics, including larger invasive size, positive LN status, and ER-positive and luminal A subtypes. Not-circumscribed margin (P <.001) and hypoechogenicity (P =.003) scores on US correlated with pathologic tumor size, and not-parallel orientation score on US correlated with histologic grade (P =.024) (Table 2). The quantitative scores for margin and echogenicity on US did not differ according to certain pathologic characteristics, including histologic grade, LN status, ER, PR, HER2 status, and tumor subtype. Multiple linear regression analysis revealed that pathologic tumor size was the only significant independent factor associated with quantitative US scores for irregular shape (P <.001) and not-circumscribed margin (P <.001).

3.3. US morphological characteristics associated with pathologic molecular subtypes

Since the pathologic size of the mass was the strongest factor associated with morphological characteristics on US, we analyzed the correlation between the quantitative score obtained using DL-CAD on US and the pathologic molecular subtype in T1-stage breast cancer to reduce the influence of tumor size on the analysis. The results of the multiple linear regression analyses are presented in Table 3. The pathologic molecular subtype independently correlated with the quantitative US scores of the irregular shape, not-circumscribed margin, and not-parallel orientation. Luminal A tumors (Fig. 2) showed higher US scores for irregular shape than TNBC (Fig. 3) and higher US scores for not-circumscribed margin and not-parallel orientation than luminal B tumors or TNBC. However, for tumors >2 cm in size, no significant variables were observed. As the pathologic size of the invasive tumor increased, the tumor tended to show a more irregular shape without a circumscribed margin on the US, regardless of the pathologic molecular subtype (Fig. 4).

Table 2

Correlations between histopathologic features and results of quantitative analysis of invasive breast cancer using DL-CAD.

Pathologic feature	Shape		Margin		Echogenicity		Orientation	
	Irregular	P-value	Not-circumscribed	P-value	Hypoechoic	P-value	Not-parallel	P-value
Invasive tumor size, cm		<.001		<.001		.003		.506
<1.0	0.32 ± 0.33		0.49 ± 0.43		0.70 ± 0.31		0.39 ± 0.41	
1.0–2.0	0.58 ± 0.31		0.77 ± 0.29		0.82 ± 0.26		0.47 ± 0.38	
>2.0	0.74 ± 0.29		0.88 ± 0.25		0.87 ± 0.21		0.44 ± 0.35	
Histologic grade		.529		.404		.054		.024
I (n = 53)	0.56 ± 0.34		0.72 ± 0.35		0.74 ± 0.32		0.53 ± 0.39	
II (n = 90)	0.62 ± 0.34		0.80 ± 0.30		0.82 ± 0.26		0.49 ± 0.39	
III (n = 139)	0.59 ± 0.33		0.76 ± 0.34		0.84 ± 0.24		0.39 ± 0.36	
LN status		.001		.097		.146		.939
Negative (n = 174)	0.55 ± 0.34		0.74 ± 0.34		0.80 ± 0.27		0.45 ± 0.39	
Positive (n = 108)	0.66 ± 0.31		0.81 ± 0.31		0.84 ± 0.24		0.45 ± 0.36	
ER status		.016		.283		.164		.004
Negative (n = 62)	0.50 ± 0.34		0.73 ± 0.33		0.86 ± 0.23		0.33 ± 0.34	
Positive (n = 220)	0.62 ± 0.33		0.78 ± 0.33		0.81 ± 0.27		0.48 ± 0.38	
PR status		.249		.374		.491		.021
Negative (n = 90)	0.56 ± 0.34		0.74 ± 0.34		0.83 ± 0.24		0.37 ± 0.34	
Positive (n = 192)	0.61 ± 0.33		0.78 ± 0.32		0.81 ± 0.27		0.48 ± 0.39	
HER2 status		.171		.617		.522		.007
Negative (n = 240)	0.61 ± 0.33		0.77 ± 0.33		0.82 ± 0.26		0.47 ± 0.38	
Positive (n = 42)	0.53 ± 0.33		0.74 ± 0.34		0.79 ± 0.28		0.31 ± 0.32	
Subtype		.048		.296		.587		.002
Luminal A (n = 144)	0.63 ± 0.32		0.80 ± 0.31		0.80 ± 0.27		0.53 ± 0.38	
Luminal B (n = 77)	0.60 ± 0.33		0.73 ± 0.36		0.82 ± 0.25		0.39 ± 0.36	
HER2 (n = 22)	0.55 ± 0.30		0.77 ± 0.29		0.85 ± 0.24		0.36 ± 0.32	
TNBC (n = 39)	0.47 ± 0.36		0.70 ± 0.35		0.86 ± 0.24		0.31 ± 0.35	

Data are presented as mean ± standard deviation.

DL-CAD = deep learning-based computer-aided diagnostic system, ER = estrogen receptor, HER2 = human epidermal growth factor receptor, LN = lymph node, PR = progesterone receptor, TNBC = triple-negative breast cancer.

4. Discussion

Our study demonstrated that quantitative morphological scores obtained using DL-CAD with B-mode breast US correlated with certain pathologic tumor characteristics, including tumor size, histologic grade, LN status, and receptor status. Among

Table 3

Multiple linear regression analysis of molecular subtypes of breast cancer associated with quantitative scores in T1 breast cancer.

Variable	B	Standard error	P-value
Irregular shape score			
Subtype			
Lum A	. . .	. . .	. . .
Lum B	−0.110	0.057	.055
HER2	−0.088	0.088	.316
TNBC	−0.307	0.074	<.001
Not-circumscribed margin score			
Subtype			
Lum A	. . .	. . .	. . .
Lum B	−0.145	0.061	.018
HER2	−0.019	0.094	.840
TNBC	−0.182	0.080	.024
Not-parallel orientation score			
Subtype			
Lum A	. . .	. . .	. . .
Lum B	−0.250	0.066	<.001
HER2	−0.170	0.102	.096
TNBC	−0.302	0.087	.001

HER2 = human epidermal growth factor receptor, Lum A = luminal A, Lum B = luminal B, TNBC = triple-negative breast cancer.

T1 stage breast cancers, luminal A tumors exhibited more irregular features with no parallel orientation on US, whereas TNBC showed rounder/more oval and parallel orientation on US.

In current clinical practice, US is a widely used non-invasive medical imaging technique for breast cancer. Breast cancer is a highly heterogeneous disease and the tumor subtype determined by IHC analysis is critical for determining the treatment options and prognosis.[42,43] However, IHC analysis has certain limitations. Owing to tumor heterogeneity, the sampling and analysis of the tumor tissue are uncertain, and visual interpretations are subjective and may lead to misinterpretations.[44,45] Radiomics is the study identifying the relationship between tumor characteristics at the cellular or genetic level and morphologic characteristics on medical images.[33,45–49] It is hypothesized that comprehensive features of the entire tumor on medical imaging could reveal predictive associations between the images and medical outcomes.[50] Breast cancer has been the primary focus of radiomics research, and in these studies, the luminal subtype tumor commonly presented as a mass with a poorly circumscribed margin on MG and US and showed posterior acoustic shadowing on US.[51,52] HER2-positive subtype tumors are often accompanied by calcifications on MG and commonly present as irregularly shaped masses on US, and washout or fast initial kinetics on MRI.[51,53] TNBC is often observed as a non-calcified, relatively circumscribed mass on the MG and a circumscribed mass with posterior acoustic enhancement on US.[51,54] Quantitative evaluation using whole-tumor histogram-based imaging features derived from apparent diffusion coefficient maps and dynamic contrast-enhanced (DCE) MR semi-quantitative maps

Figure 2. Breast ultrasound image of a 67-year-old woman showing an 11-mm luminal A subtype, grade II invasive carcinoma, not otherwise specified. On the grayscale ultrasound image, the region of interest is drawn (in red color) along the border of the mass using the deep learning-based computer-aided diagnostic system (A). The raw data for quantitative scores are irregular shape, 0.0915; not-circumscribed margin, 0.637; hypoechoic echogenicity, 0.959; and not-parallel orientation, 0.971. The gross photograph of tumor specimen (white arrow, B) and low-power hematoxylin and eosin (H&E, ×7) slide of this tumor (C) revealed the irregular shape and not-circumscribed margin of this tumor (* pectoralis muscle under the lesion).

or multiparametric MRI have provided useful information for differentiating TNBC from other subtypes on MRI.[55,56]

Thus far, radiomics research using US has been limited owing to its operator dependency and subjective interpretation characteristics. The recent development of DL-CAD enabled the morphological analysis of breast mass based on the raw data

of quantitative scores for the BI-RADS lexicon. Several studies have reported that DL-CAD can help improve the diagnostic performance, especially accuracy and specificity, of breast US for distinguishing benign from malignant lesions.[24,26,56,57] However, to the best of our knowledge, no study has analyzed raw data itself, driven by DL-CAD, to quantify the morphological
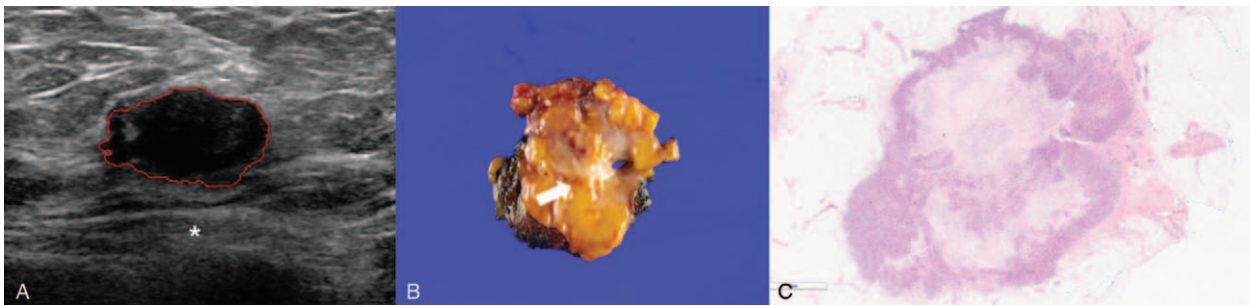

Figure 3. Breast ultrasound image of a 47-year-old woman with a 15-mm TNBC subtype, grade III invasive carcinoma, not otherwise specified NOS. On the grayscale ultrasound image, the region of interest is drawn (in red color) along the border of the mass using the deep learning-based computer-aided diagnostic system by DL-CAD (A). The raw data for quantitative scores are irregular shape, 0.020; not- circumscribed margin, 0.019; hypoechoic echogenicity, 0.990; not-parallel orientation, 0.004. The gross photograph of tumor specimen (white arrow, B) and low-power hematoxylin and eosin (H&E, ×7) slide of this tumor (C) revealed the oval shape and circumscribed margin of this tumor (* pectoralis muscle under the lesion). DL-CAD = deep learning-based computer-aided diagnosis, NOS = not otherwise specified.
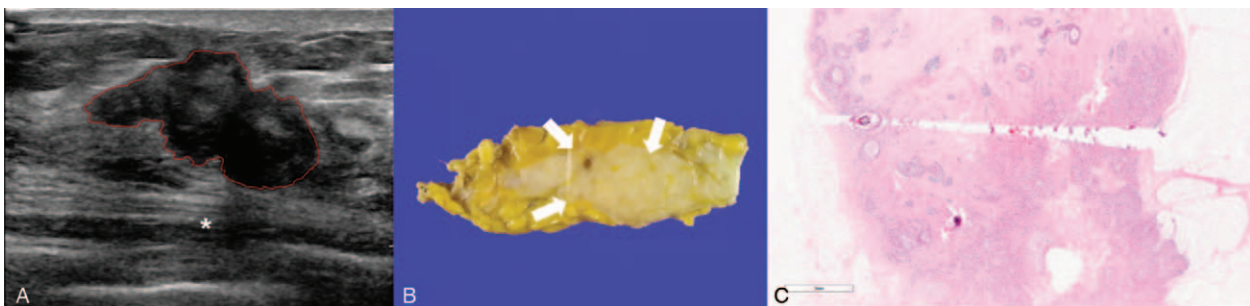

Figure 4. Breast ultrasound image of a 73-year-old woman with a 27-mm TNBC subtype, grade III invasive carcinoma, not otherwise specified NOS. On the grayscale ultrasound image, the region of interest is drawn (in red color) along the border of the mass by using the deep learning-based computer-aided diagnostic system DL-CAD. The raw data for quantitative scores are irregular shape, 0.991; not-circumscribed margin, 0.998; hypoechoic echogenicity, 0.957; not-parallel orientation, 0.423. The gross photograph of tumor specimen (white arrows, B) and low-power hematoxylin and eosin (H&E, ×7) slide of this tumor (C) revealed the irregular shape and not-circumscribed margin of this tumor. Since the large size of the tumor, the entire morphology of tumor was not included in the one same slide (* pectoralis muscle under the lesion). DL-CAD = deep learning-based computer-aided diagnosis, NOS = not otherwise specified.

characteristics of breast cancers. Kim et al[58] analyzed the diagnostic performance of breast US using quantitative variables, but the quantitative variables in that study were width, height, height/width ratio, area, and depth. This is the first study focusing on the correlation between molecular subtype and sonographic features of breast cancer using quantitative analysis by DL-CAD with breast US.

Our DL-CAD-based results are consistent with those of previous studies revealing that luminal subtype tumors tend to present as a mass with a poorly circumscribed margin, HER2-positive subtype as an irregular mass with a not-circumscribed margin, and TNBC as a distinct mass with a circumscribed margin on US when the tumor size is <2 cm.[51] However, an interesting finding was that as the pathologic size of the invasive tumor increased, the tumor tended to show a more irregular shape without a circumscribed margin on the US regardless of the molecular subtype, which meant that the molecular subtype of the tumor was significantly correlated with the ultrasonographic morphological characteristics only when the tumor size was below the T1 stage. Thus, the imaging phenotypes of breast cancer should be cautiously interpreted based on tumor size.

Our study had some limitations. First, this was a retrospective study from a single center with a limited number of cases. We used representative still images stored in the PACS system instead of real-time ultrasonographic examinations during image analysis by DL-CAD; thus, there is the possibility of selection bias and reader variability in determining the representative images of breast cancer. Second, non-mass lesions were not included in this study. Third, our findings do not suggest a clinically useful cutoff value by DL-CAD to assign tumor molecular subtypes using US images.

In conclusion, using DL-CAD, we demonstrated that quantitative analysis of the morphological characteristics of breast cancers on US correlated with the histopathologic features and could provide useful information regarding the imaging phenotypes of breast cancer.

Acknowledgments

Author contributions

Conceptualization: Jung Min Chang.
Data curation: Young Seon Kim, Seung Eun Lee, Soo-Yeon Kim, Young Kyung Bae.
Formal analysis: Young Seon Kim, Seung Eun Lee, Jung Min Chang, Soo-Yeon Kim, Young Kyung Bae.
Funding acquisition: Jung Min Chang, Young Seon Kim.
Investigation: Young Seon Kim, Seung Eun Lee, Soo-Yeon Kim.
Methodology: Young Seon Kim.
Supervision: Jung Min Chang.
Visualization: Young Seon Kim, Young Kyung Bae.
Writing – original draft: Young Seon Kim.
Writing – review & editing: Young Seon Kim, Jung Min Chang.

References

[1] Bray F, Ferlay J, Soerjomataram I, Siegel RL, Torre LA, Jemal A. Global cancer statistics 2018: GLOBOCAN estimates of incidence and mortality worldwide for 36 cancers in 185 countries. CA Cancer J Clin 2018;68:394–424.

[2] Parise CA, Bauer KR, Brown MM, Caggiano V. Breast cancer subtypes as defined by the estrogen receptor (ER), progesterone receptor (PR), and the human epidermal growth factor receptor 2 (HER2) among women with invasive breast cancer in California, 1999–2004. Breast J 2009;15:593–602.

[3] Zhu X, Ying J, Wang F, Wang J, Yang H. Estrogen receptor, progesterone receptor, and human epidermal growth factor receptor 2 status in invasive breast cancer: a 3,198 cases study at National Cancer Center, China. Breast Cancer Res Treat 2014;147:551–5.

[4] Aerts HJ. The potential of radiomic-based phenotyping in precision medicine: a review. JAMA Oncol 2016;2:1636–42.

[5] Colen R, Foster I, Gatenby R, et al. NCI Workshop Report: clinical and computational requirements for correlating imaging phenotypes with genomics signatures. Transl Oncol 2014;7:556–69.

[6] Gillies RJ, Kinahan PE, Hricak H. Radiomics: images are more than pictures, they are data. Radiology 2016;278:563–77.

[7] Choi JS, Han BK, Ko ES, et al. Effect of a deep learning framework-based computer-aided diagnosis system on the diagnostic performance of radiologists in differentiating between malignant and benign masses on breast ultrasonography. Korean J Radiol 2019;20:749–58.

[8] Park HJ, Kim SM, La Yun B, et al. A computer-aided diagnosis system using artificial intelligence for the diagnosis and characterization of breast masses on ultrasound: Added value for the inexperienced breast radiologist. Medicine (Baltimore) 2019;98:e14146.

[9] Surov A, Meyer HJ, Wienke A. Associations between PET parameters and expression of Ki-67 in breast cancer. Transl Oncol 2019;12:375–80.

[10] Li H, Zhu Y, Burnside ES, et al. Quantitative MRI radiomics in the prediction of molecular classifications of breast cancer subtypes in the TCGA/TCIA data set. NPJ Breast Cancer 2016;2:16012.

[11] Zhu Y, Li H, Guo W, et al. Deciphering genomic underpinnings of quantitative MRI-based radiomic phenotypes of invasive breast carcinoma. Sci Rep 2015;5:17787.

[12] Burnside ES, Drukker K, Li H, et al. Using computer-extracted image phenotypes from tumors on breast magnetic resonance imaging to predict breast cancer pathologic stage. Cancer 2016;122:748–57.

[13] Han DS, Wu WT, Hsu PC, Chang HC, Huang KC, Chang KV. Sarcopenia is associated with increased risks of rotator cuff tendon diseases among community-dwelling elders: a cross-sectional quantitative ultrasound study. Front Med (Lausanne) 2021;8:630009.

[14] Wu WT, Chen LR, Chang HC, Chang KV, Özçakar L. Quantitative ultrasonographic analysis of changes of the suprascapular nerve in the aging population with shoulder pain. Front Bioeng Biotechnol 2021; 9:640747.

[15] Vourtsis A, Berg WA. Breast density implications and supplemental screening. Eur Radiol 2019;29:1762–77.

[16] Alvarez S, Añorbe E, Alcorta P, López F, Alonso I, Cortés J. Role of sonography in the diagnosis of axillary lymph node metastases in breast cancer: a systematic review. AJR Am J Roentgenol 2006;186:1342–8.

[17] Tucker NS, Cyr AE, Ademuyiwa FO, et al. Axillary ultrasound accurately excludes clinically significant lymph node disease in patients with early stage breast cancer. Ann Surg 2016;264:1098–102.

[18] Berg WA, Gilbreath PL. Multicentric and multifocal cancer: whole-breast US in preoperative evaluation. Radiology 2000;214:59–66.

[19] Graham LJ, Shupe MP, Schneble EJ, et al. Current approaches and challenges in monitoring treatment responses in breast cancer. J Cancer 2014;5:58–68.

[20] Forouhi P, Walsh JS, Anderson TJ, Chetty U. Ultrasonography as a method of measuring breast tumour size and monitoring response to primary systemic treatment. Br J Surg 1994;81:223–5.

[21] LeCun Y, Bengio Y, Hinton G. Deep learning. Nature 2015;521:436–44.

[22] Sahiner B, Chan HP, Roubidoux MA, et al. Malignant and benign breast masses on 3D US volumetric images: effect of computer-aided diagnosis on radiologist accuracy. Radiology 2007;242:716–24.

[23] van Zelst JCM, Tan T, Platel B, et al. Improved cancer detection in automated breast ultrasound by radiologists using computer aided detection. Eur J Radiol 2017;89:54–9.

[24] Cho E, Kim EK, Song MK, Yoon JH. Application of computer-aided diagnosis on breast ultrasonography: evaluation of diagnostic performances and agreement of radiologists according to different levels of experience. J Ultrasound Med 2018;37:209–16.

[25] Doi K. Computer-aided diagnosis in medical imaging: historical review, current status and future potential. Comput Med Imaging Graph 2007;31:198–211.

[26] Kim K, Song MK, Kim EK, Yoon JH. Clinical application of S-Detect to breast masses on ultrasonography: a study evaluating the diagnostic performance and agreement with a dedicated breast radiologist. Ultrasonography 2017;36:3–9.

[27] Nie K, Chen JH, Yu HJ, Chu Y, Nalcioglu O, Su MY. Quantitative analysis of lesion morphology and texture features for diagnostic prediction in breast MRI. Acad Radiol 2008;15:1513–25.

[28] Wang TC, Huang YH, Huang CS, et al. Computer-aided diagnosis of breast DCE-MRI using pharmacokinetic model and 3-D morphology analysis. Magn Reson Imaging 2014;32:197–205.

[29] Luo WQ, Huang QX, Huang XW, Hu HT, Zeng FQ, Wang W. Predicting breast cancer in breast imaging reporting and data system (BI-RADS) ultrasound category 4 or 5 lesions: a nomogram combining radiomics and BI-RADS. Sci Rep 2019;9:11921.

[30] Waugh SA, Purdie CA, Jordan LB, et al. Magnetic resonance imaging texture analysis classification of primary breast cancer. Eur Radiol 2016;26:322–30.

[31] Wu T, Li J, Wang D, et al. Identification of a correlation between the sonographic appearance and molecular subtype of invasive breast cancer: a review of 311 cases. Clin Imaging 2019;53:179–85.

[32] Zheng FY, Lu Q, Huang BJ, et al. Imaging features of automated breast volume scanner: correlation with molecular subtypes of breast cancer. Eur J Radiol 2017;86:267–75.

[33] Guo Y, Hu Y, Qiao M, et al. Radiomics analysis on ultrasound for prediction of biologic behavior in breast invasive ductal carcinoma. Clin Breast Cancer 2018;18:e335–44.

[34] Çelebi F, Pilancı KN, Ordu Ç, et al. The role of ultrasonographic findings to predict molecular subtype, histologic grade, and hormone receptor status of breast cancer. Diagn Interv Radiol 2015;21:448–53.

[35] Elston CW, Ellis IO. Pathological prognostic factors in breast cancer. I. The value of histological grade in breast cancer: experience from a large study with long-term follow-up. Histopathology 1991;19:403–10.

[36] Hammond ME, Hayes DF, Dowsett M, et al. American Society of Clinical Oncology/College Of American Pathologists guideline recommendations for immunohistochemical testing of estrogen and progesterone receptors in breast cancer. J Clin Oncol 2010;28:2784–95.

[37] Dowsett M, Nielsen TO, A'Hern R, et al. Assessment of Ki67 in breast cancer: recommendations from the International Ki67 in Breast Cancer working group. J Natl Cancer Inst 2011;103:1656–64.

[38] Goldhirsch A, Winer EP, Coates AS, et al. Personalizing the treatment of women with early breast cancer: highlights of the St Gallen International Expert Consensus on the Primary Therapy of Early Breast Cancer 2013. Ann Oncol 2013;24:2206–23.

[39] Kim S, Choi Y, Kim E, et al. Deep learning-based computer-aided diagnosis in screening breast ultrasound to reduce false-positive diagnoses. Sci Rep 2021;11:395.

[40] Park VY, Han K, Seong YK, et al. Diagnosis of thyroid nodules: performance of a deep learning convolutional neural network model vs. radiologists. Sci Rep 2019;9:17843.

[41] Han S, Kang HK, Jeong JY, et al. A deep learning framework for supporting the classification of breast lesions in ultrasound images. Phys Med Biol 2017;62:7714–28.

[42] de Ronde JJ, Hannemann J, Halfwerk H, et al. Concordance of clinical and molecular breast cancer subtyping in the context of preoperative chemotherapy response. Breast Cancer Res Treat 2010;119:119–26.

[43] Sørlie T, Perou CM, Tibshirani R, et al. Gene expression patterns of breast carcinomas distinguish tumor subclasses with clinical implications. Proc Natl Acad Sci U S A 2001;98:10869–74.

[44] Yip SS, Aerts HJ. Applications and limitations of radiomics. Phys Med Biol 2016;61:R150–66.

[45] Yang X, Knopp MV. Quantifying tumor vascular heterogeneity with dynamic contrast-enhanced magnetic resonance imaging: a review. J Biomed Biotechnol 2011;2011:732848.

[46] Aerts HJ, Velazquez ER, Leijenaar RT, et al. Decoding tumour phenotype by noninvasive imaging using a quantitative radiomics approach. Nat Commun 2014;5:4006.

[47] Cho GY, Moy L, Kim SG, et al. Evaluation of breast cancer using intravoxel incoherent motion (IVIM) histogram analysis: comparison with malignant status, histological subtype, and molecular prognostic factors. Eur Radiol 2016;26:2547–58.

[48] Lee SH, Park H, Ko ES. Radiomics in breast imaging from techniques to clinical applications: a review. Korean J Radiol 2020;21:779–92.

[49] Oakden-Rayner L, Carneiro G, Bessen T, Nascimento JC, Bradley AP, Palmer LJ. Precision radiology: predicting longevity using feature engineering and deep learning methods in a radiomics framework. Sci Rep 2017;7:1648.

[50] Kumar V, Gu Y, Basu S, et al. Radiomics: the process and the challenges. Magn Reson Imaging 2012;30:1234–48.

[51] Cho N. Molecular subtypes and imaging phenotypes of breast cancer. Ultrasonography 2016;35:281–8.

[52] Shin HJ, Kim HH, Huh MO, et al. Correlation between mammographic and sonographic findings and prognostic factors in patients with node-negative invasive breast cancer. Br J Radiol 2011;84:19–30.

[53] Elias SG, Adams A, Wisner DJ, et al. Imaging features of HER2 overexpression in breast cancer: a systematic review and meta-analysis. Cancer Epidemiol Biomarkers Prev 2014;23:1464–83.

[54] Dogan BE, Turnbull LW. Imaging of triple-negative breast cancer. Ann Oncol 2012;23(suppl):vi23–9.

[55] Xie T, Zhao Q, Fu C, et al. Differentiation of triple-negative breast cancer from other subtypes through whole-tumor histogram analysis on multiparametric MR imaging. Eur Radiol 2019;29:2535–44.

[56] Montemezzi S, Camera L, Giri MG, et al. Is there a correlation between 3T multiparametric MRI and molecular subtypes of breast cancer? Eur J Radiol 2018;108:120–7.

[57] Choi JH, Kang BJ, Baek JE, Lee HS, Kim SH. Application of computer-aided diagnosis in breast ultrasound interpretation: improvements in diagnostic performance according to reader experience. Ultrasonography 2018;37:217–25.

[58] Kim Y, Kang BJ, Lee JM, Kim SH. Comparison of the diagnostic performance of breast ultrasound and CAD using BI-RADS descriptors and quantitative variables. Iran J Radiol 2019;16:e67729.